symmetry

IMPACT FACTOR 2.7

CITESCORE 4.9

Article

Retarded Gravity in Disk Galaxies

Yuval Glass, Tomer Zimmerman and Asher Yahalom

MDPI

https://doi.org/10.3390/sym16040387

symmetry

MDPI

Article

Retarded Gravity in Disk Galaxies

Yuval Glass [1], Tomer Zimmerman [2] and Asher Yahalom [1,3,*]

[1] Department of Electrical & Electronic Engineering, Faculty of Engineering, Ariel University, Ariel 40700, Israel
[2] Department of Physics, Faculty of Natural Sciences, Ariel University, Ariel 40700, Israel
[3] Center for Astrophysics, Geophysics, and Space Sciences (AGASS), Ariel University, Ariel 40700, Israel
* Correspondence: asya@ariel.ac.il; Tel.: +972-54-7740294

Abstract: Disk galaxies have a typical dimension of a few tens of kiloparsecs. It follows from the theory of general relativity that any signal originating from the galactic center will be noticed at the outskirts of the galaxy only tens of thousands of years later. This retardation effect, however, is absent in modelling used to calculate rotation curves throughout entire galaxies and their external gas. The considerable differences between Newtonian predictions and observed velocities are currently removed either by assuming dark matter or by suggesting various modifications to the laws of gravity, MOND being a long standing alternative to Newtonian gravity. In previous papers we have shown that by applying general relativity in a rigorous fashion, without neglecting retardation, one can explain the rotational velocities of galactic matter without modifying gravity or adding dark matter. Moreover, it was shown that dark matter effects, as they appear in gravitational lensing, the Tully-Fisher relation, and mass estimations based on the virial theorem could also be explained as retarded-gravity effects. It must be noted, however, that the proposed theory relies on the existence of a mass flow (of a changing rate) into the galaxy; a requirement that was not directly observed. In the original paper on the subject only one galaxy (M33) was analysed in detail. This was later amended with a published study of eleven galaxies. Here we give a more comprehensive retardation analysis of 143 galaxies of different types from the SPARC Galaxy collection. We show that in most cases we obtain very accurate fits to the data.

Keywords: dark matter; MOND; retardation; general relativity

Citation: Glass, Y.; Zimmerman, T.; Yahalom, A. Retarded Gravity in Disk Galaxies. *Symmetry* **2024**, *16*, 387. https://doi.org/10.3390/sym16040387

Academic Editor: Kazuharu Bamba

Received: 18 February 2024
Revised: 9 March 2024
Accepted: 13 March 2024
Published: 26 March 2024

1. Introduction

From an empirical perspective general relativity (GR) is known to be verified by many different types of observations [1–5]. However, Einstein's general relativity is currently in a rather difficult position. It has much support from observational evidence, but it also faces challenges in the domain of cosmology. The observational verifications it has gained in both cosmology and astrophysics rely on the existence of unconfirmed ingredients: dark matter and dark energy. Those were postulated in order to achieve success on the larger scales, i.e., galaxies, clusters of galaxies and the universe as a whole. In a lot of cases, however, the unconfirmed ingredients are used while at the same time practitioners neglect a major ingredient of general relativity, the phenomenon of retardation, which negates Newtonian action at a distance.

Indeed, the dark matter enigma has not only been with the astronomical community since the 1930s (or perhaps even since the 1920s when it was known as the question of missing mass), but it has also become prevalent as more dark matter has had to be postulated on larger scales as those scales were scrutinized. A very detailed and costly forty-years underground and accelerator search failed to prove its existence. The dark matter enigma has become even more problematic in recent years as the Large Hadron Collider failed to find any supersymmetric particles, not only the astro-particle community's preferred form of dark matter.

As early as 1933, Zwicky noted that a group of galaxies within the Comma Cluster have velocities that are significantly higher than that predicted by virial calculations based on Newtonian theory [6,7]. His calculations showed that the amount of matter required to account for the velocities could be 400 times greater than that of visible matter (this was later mitigated somewhat). In a recent paper we showed that the retarded gravity version of the virial theory [8] may yield better estimates of the mass.

In 1959, on a smaller galactic scale, Volders observed that stars in the outer rims of a nearby spiral galaxy (M33) do not move as they should [9]. That is to say that the velocities do not decrease as $1/\sqrt{r}$. This discrepancy was further established in later years. During the seventies Rubin and Ford [10–12] have shown that for a rather large sample of spiral galaxies the velocities at the outer rim of galaxies do not decrease. Rather, in the general case, they attain a plateau (or continue increasing) at some velocity different for each galaxy (see [13–15]). In previous works it was shown that such velocity curves can be deduced directly from GR if retardation effect is taken into account. The derivation of the retardation effect is described in previous publications [16–20].

The mechanism is strongly connected to the dynamics of the matter density inside the galaxy, or more specifically to the densities' second derivative. The density can change due to the depletion of gas in the galaxies surrounding (in which case the second derivative of the galaxies' total mass is negative [18]) but can also be affected by dynamical processes involving star formation and supernovae explosions [16,17]. It was determined that all possible processes can be captured by three different length scales: the typical length of the density gradient, the typical length of the velocity field gradient and the dynamical length scale. It is the shortest among those length scales that determine the significance of retardation [21].

The famous relation of [22] connecting the baryonic mass of a galaxy to the fourth power of its rim velocity can also be deduced from retarded gravity [23]. Retarded gravity not only affect slow-moving particles but also photons. Although the mathematical analysis is slightly different in both cases [21,24], it is concluded that the apparent "dark mass" must be the same as in the galactic rotation curves.

The current situation in cosmology is alarming enough to contemplate the possibility that the current prevailing paradigm might at least be reconsidered. We mention a few difficulties that add doubt to the common paradigm. First, in order to comply with said observations and structure formation simulations a list of properties has been attributed to dark matter [6]. However, to date, 50 years since its inception, DM has not been observed nor could any known particles be identified with its particular properties.

Second, dark matter simulations are notorious for having a core–cusp problem. Navarro–Frenk–White (NFW) [25] is the prevalent dark matter profile used today to describe galactic rotation curves. It is directly derived from Cold Dark Matter (CDM) simulations. However, NFW faces major difficulties in low surface-brightness galaxies (LSBs). Its predictions for rotational velocities and actual observations often appear to be in tension. More specifically, an NFW profile predicts a "cuspy" inner region for a dark halo (i.e., the inner density is changing fast) while observations prefer a "core-like" (approximately constant density) behavior. Many attempts have been made over the years to resolve this tension but with limited success.

Third, the law of Sancisi [26] is a significant empirical deduction. It challenges dark halos of many types. The content of the law states that for "each and every property of the luminosity profile there is a corresponding indication in the rotation curve and vice versa". To put this in different words, minute changes in the luminous matter profile ("features") are identified in the rotation curve. This is unexpected from a dark-matter perspective: the dark halo is more massive than baryons according to standard modeling. It thus follows that in prevalent areas of the galaxy, small disturbances in the baryonic density are of no consequence to the modeled rotational curve, as opposed to empirical data.

Thus there is indeed room for the present suggestion. Unlike other theories such as Milgrom's MOND [27], Mannheim's Conformal Gravity [28,29] or Moffat's MOG [30], the current approach does not require modifications to general relativity. It seeks to replace

dark matter with effects within the standard General Relativity itself. Notice, however, that the connection between retardation and MOND was recently elucidated [31], showing in what sense low acceleration MOND criteria can be derived from retardation theory and how MOND interpolation function can be a good approximation to retarded gravity.

We emphasize that appreciable retardation effects do not require that velocities of matter in the galaxy are high (although this may help). In fact, the vast majority of galactic bodies (stars, gas) are slow with respect to the speed of light. To obtain appreciable retardation effects what is needed is a small typical gradient scale with respect to the size of the system [21]. It was shown that retardation effects may become significant even at low speeds, provided that the distance over a typical length scale is large enough.

The purpose of this study is to establish the empirical basis for the retarded gravity theory. It expands previous work that analyzed eleven galaxies [17] to the current application of a larger sample of 143 galaxies. These 143 galaxies that originated from the SPARC Galaxy collection are of different types, sizes and luminosities. We show that in most cases, we obtain excellent fits to the data.

2. Retardation Effects beyond the Newtonian Approximation

The mathematical similarities between GR and Electromagnetic (EM) theory have not gone unnoticed. While exact solutions of GR have proven challenging due to the non-linear nature of the Einstein equations, within the weak field approximation the equations are linear, therefore superposable, yielding a Retarded Potential [5,32] similar to that of electromagnetic theory [33,34]. The form of the equations in both cases is related to the structure of the constant Lorentzian metric [35,36].

The retarded gravitational potential ϕ is given by:

$$\phi = -G \int \frac{\rho(\vec{x}', t - \frac{R}{c})}{R} d^3x' \tag{1}$$

with the same (common) notations as in [18].

When focusing on the far field solutions of the Retarded Potential (Equation (1)) in a similar manner to EM theory, the exciting possibility of gravitational waves, for example, rises [5,32]. Since the far field approach is not suitable within galaxies, or even at their edges, as the galaxy itself is the source system, retardation theory [18–21,23,24] focuses on the near field solutions, yielding a near field regime.

When studying far-field approximations of the retarded potential depicted in Equation (1) in a way that resembles electromagnetism, the interesting possibility of gravitational waves (for example) is deduced [5,32]. Since the far field approach is not suitable within galaxies, or even at their edges, as the galaxy itself is the source system, retardation theory [18–21,23,24] focuses on the near field solutions, yielding a near field regime.

Using Equation (1), one may derive the force per unit mass:

$$\begin{aligned} \vec{F} &= -\vec{\nabla}\phi = \vec{F}_{Nr} + \vec{F}_r \\ \vec{F}_{Nr} &= -G \int \frac{\rho(\vec{x}', t - \frac{R}{c})}{R^2} \hat{R} d^3x', \qquad \hat{R} \equiv \frac{\vec{R}}{R} \\ \vec{F}_r &\equiv -\frac{G}{c} \int \frac{\rho^{(1)}(\vec{x}', t - \frac{R}{c})}{R} \hat{R} d^3x', \qquad \rho^{(n)} \equiv \frac{\partial^n \rho}{\partial t^n}. \end{aligned} \tag{2}$$

Thus a retarded potential does not simply imply a retarded Newtonian force $\vec{F}_{Nr}$, but in addition a pure "retardation" force $\vec{F}_r$ which decreases more slowly than the Newtonian force with distance. We emphasize that this result is independent of any perturbation expansion in the delay time $\frac{R}{c}$ as was done in [18]. However, the perturbation expansion does shed some light on the nature of those force terms as is explained below.

The duration $\frac{R}{c}$ may be tens of thousands of years, yet short with respect to the duration in which the galactic density changes considerably. Therefore, we write a Taylor expansion for the density:

$$\rho(\vec{x}', t - \frac{R}{c}) = \sum_{n=0}^{\infty} \frac{1}{n!} \rho^{(n)}(\vec{x}', t)(-\frac{R}{c})^n. \tag{3}$$

By inserting Equation (3) into Equation (1), we obtain

$$\begin{aligned} \phi &= \phi_2 + \phi_{(n>2)} \\ \phi_2 &= -G \int \frac{\rho(\vec{x}', t)}{R} d^3x' + \frac{G}{c} \int \rho^{(1)}(\vec{x}', t) d^3x' - \frac{G}{2c^2} \int R\rho^{(2)}(\vec{x}', t) d^3x' \\ \phi_{(n>2)} &= -G \sum_{n=3}^{\infty} \frac{(-1)^n}{n! c^n} \int R^{n-1} \rho^{(n)}(\vec{x}', t) d^3x' \end{aligned} \tag{4}$$

The Newtonian potential is the first term, the second term has null contribution, and the third term is the lower order correction to the Newtonian theory:

$$\phi_r = -\frac{G}{2c^2} \int R\rho^{(2)}(\vec{x}', t) d^3x' \tag{5}$$

Equation (4) describes a Taylor expansion, and thus, is only applicable for a limited distance specified by the infinite sum convergence:

$$R < c\, T_{max} \equiv R_{max} \tag{6}$$

Thus, it follows that the approximation is only valid in the near field; this is in contrast with the different far-field approximation of gravitational [2,37,38]. The applicability of the formula is much more limited when a second-order expansion is considered [18].

If $n > 2$ terms can be neglected, the total force per unit mass can be approximated by

$$\begin{aligned} \vec{F} &\simeq \vec{F}_N + \vec{F}_{ar} \\ \vec{F}_N &= -\vec{\nabla}\phi_N = -G \int \frac{\rho(\vec{x}', t)}{R^2} \hat{R} d^3x', \qquad \hat{R} \equiv \frac{\vec{R}}{R} \\ \vec{F}_{ar} &\equiv -\vec{\nabla}\phi_r = \frac{G}{2c^2} \int \rho^{(2)}(\vec{x}', t) \hat{R} d^3x'. \end{aligned} \tag{7}$$

$\vec{F}_N$ is purely Newtonian (no retardation); please see [20] for additional details. The insignificance of the term proportional to $\frac{1}{c}$ is quite remarkable and also happens in the corresponding electromagnetic problem [39]. If $r = |\vec{x}| \to \infty$, it follows that $\hat{R} \simeq \frac{\vec{x}}{|\vec{x}|} \equiv \hat{r}$ and

$$\vec{F}_{ar} = \frac{G}{2c^2} \hat{r} \int \rho^{(2)}(\vec{x}', t) d^3x' = \frac{G}{2c^2} \hat{r} \ddot{M}, \qquad \ddot{M} \equiv \frac{d^2M}{dt^2}. \tag{8}$$

The above approximation is rather useful as the dominant retardation effect usually occurs outside the main mass of the galaxy. As the galaxy gravitates gas from the intergalactic medium, its mass increases, and thus, $\dot{M} > 0$; however, the gas in the intergalactic medium is depleted, and thus, the rate at which the mass is obtained decreases, that is, $\ddot{M} < 0$. This is of course a much oversimplified description of the overall situation in which star formation and supernovae explosions affect the mass accretion rate of the galaxy.

Thus, in the galactic case:

$$\vec{F}_{ar} = -\frac{G}{2c^2} |\ddot{M}| \hat{r} \tag{9}$$

and the retardation force is attractive.

$\vec{F}_N$ is certainly attractive; however, the retardation force $\vec{F}_r$ may be either attractive or repulsive. Newton's force is proportional to $\frac{1}{R^2}$; in contrast, the force implied by retardation

is not a function of the radial distance provided the approximation of Equation (3) is valid. For short distances, Newtonian forces are surely greater; however, for far radial distances, the retardation force becomes dominant. The Newtonian force is negligible for distances significantly larger compared with the distance:

$$R \gg R_r \equiv c\Delta t \tag{10}$$

Δt is related to the temporal second-order derivative of ρ. Provided that $R \ll R_r$, retardation forces can be ignored and only the Newtonian force should be considered, as is done correctly in the solar system. For the outer parts of galaxies, neither force seems to be negligible, and both have to be considered.

It can be claimed that since for the galaxy $\ddot{M} < 0$ and the total mass is conserved it must be that $\ddot{M} > 0$ for the matter outside the galaxy. Therefore, retardation forces $\vec{F}_{ar}$ inside and outside the galaxy should cancel out. However, note that Equation (7) is only valid when $\frac{R}{c}$ is small. This is certainly not the case when the rest of the universe outside the galaxy is taken into account. In [20], we showed that a retardation force exists regardless of whether Equation (3) is expanded.

Since for a typical galaxy, $\ddot{M} < 0$ and the system's total mass is conserved, it follows that $\ddot{M} > 0$ for the intergalactic gas, and thus, $\vec{F}_{ar}$ in the galaxy and outside the galaxy should cancel each other. However, note that Equation (7) is only valid when $\frac{R}{c}$ is small, which is certainly not the case when the rest of the universe outside the galaxy is considered. In [20], it is shown that a retardation force is significant even if the expansion given by Equation (3) is not applicable.

3. Methodological Remarks

Our goal was to fit a significant number of rotation curves using the retardation model. In order to accomplish this goal, we relied on the SPARC database of [40]. The database includes galaxies with extended 21-cm rotation curves spanning a large range of luminosities and radii. Galactic rotation curves are calculated by the formula:

$$\frac{v_\theta^2}{r} = F, \tag{11}$$

where v_θ is the rotational velocity, r is the distance from the galactic center and F is the total force in the inward direction.

In our case, the force is the combined effect of two components, thus:

$$\frac{v_\theta^2}{r} = F = F_N + F_{ar} = F_N + \frac{G}{2c^2}|\ddot{M}|, \tag{12}$$

where F_N is the Newtonian term and F_{ar} is the retarded-gravity term. In the above we use the approximation given in Equation (9) which will suffice in most cases, and allows automatization of the curve fitting process. However, to obtain high quality results, more detailed modelling of the density is required as described in [18].

Each observed rotation curve in the database was accompanied by the Newtonian velocity components of its stellar disk $v_{disk}(r) = \sqrt{rF_{Ndisk}}$, galactic bulge $v_{bulge}(r) = \sqrt{rF_{Nbulge}}$ and gaseous disk $v_{gas}(r) = \sqrt{rF_{Ngas}}$. These corresponded to the expected circular Newtonian velocities (i.e., the models) produced by each galactic component. For simplicity, in this study, we selected only the galaxies with no bulge components.

Let us now take a closer look at our model and discuss its different terms. Equation (12) can be rewritten in the following form:

$$v_{predicted}(r) = \sqrt{(M/L) \cdot v_{disk}^2(r) + v_{gas}^2(r) + \frac{Gr}{2c^2}|\ddot{M}|}, \tag{13}$$

where M/L is the stellar disk mass-to-light ratio, which signifies the fact that mass is not observed directly but is derived from the (absolute) luminosity of the galaxy. The model is, therefore, dependent on two free parameters: M/L and $|\ddot{M}|$ (v_{disk} corresponds to a disk velocity contribution for a mass-to-light of unity).

Let us briefly discuss the different velocity components. The publicly-available velocity distribution $v_{disk}(r)$ of each galaxy (i.e., prediction for the disk) was numerically obtained from the corresponding light distribution of that galaxy. The light distribution of a galaxy traces the stellar mass distribution. Therefore, given the light distribution (combined with the chosen M/L), the gravitational and velocity fields of the disk component could be derived. The publicly-available velocity distribution $v_{gas}(r)$ of each galaxy was numerically derived from the observed neutral hydrogen. The gaseous disk component may also contribute to the overall velocity, especially in low-luminosity galaxies. The disk and gas components of each galaxy, that is, $v_{disk}(r)$ and $v_{gas}(r)$, are available online in [40] as numerical data files. Sanders and McGaugh [41] provide more details on the extraction of these components.

The fit (i.e., Equation (13)) was obtained using the least-squares method. We searched for the values of M/L and $|\ddot{M}|$ that minimized χ^2 in each galaxy; that is to say, the best fit values of these two parameters. This was done through a dedicated MATLAB script that searched for the values iteratively. It started with a two-dimensional grid of initial guesses. From each point on the grid, it tried to find a close local minimum. It then combined the results to obtain a global minimum. In some cases, the M/L value was found from the inner Newtonian part of the rotation curve, simplifying the parameter search.

4. Rotation Curves

The rotation curves of the 143 galaxies from the SPARC Galaxy collection are given in Appendix A. It is worth noting that the SPARC Galaxy collection contains 175 galaxies, but for the sake of simplicity, we took galaxies in which the size of the bulge was very small so that we could neglect the height of the galaxy in the z-axis in relation to the size of the galaxy in the x–y plane. Moreover, the notion that the mass-to-light parameter is constant across a galaxy is more suitable in bulge-less galaxies. We performed a fitting for each galaxy by finding two parameters: the mass-to-light ratio and absolute value of the second derivative of the mass. We arranged the sample results according to the Hubble morphological sequence, which is a method of galaxy classification based on their appearance.

In the plots, the blue line describes the Newtonian contribution, the green line describes the contribution resulting from the retardation, the red line describes the joint contribution of the Newtonian force and the retardation force, and black dots describe the SPARC data. In addition, above each plot, we indicate the values of the mass-to-light ratio, the second mass derivative and the total mass of the galaxy. The total mass was calculated from the M/L that was found and was not a free parameter. The results of this procedure are shown in Appendix A. We are not considering here an in-depth statistical analysis of the results. However, it is clear from the plots that most rotation curves are fitted quite well, although the model includes only one extra free parameter.

5. Correlations

In this study, we attempted to address the missing mass problem by fitting the rotation curves of 143 galaxies using the retardation model. Summarized tables of the relevant galactic parameters are also given in Appendix B. We emphasize that the additional free parameter of the retardation model is the magnitude of the second derivative of the mass. This parameter represents the novelty of the current approach. Therefore, it would be interesting to search for correlations between this parameter and other galaxy parameters (e.g., mass, radius, type). Importantly, we found no correlations between the size of the second derivative of the mass and the radius or mass of the galaxies, nor was there any correlation between the size of the second derivative and the type of the galaxy according to the Hubble classification. This could indicate that our proposed solution does not depend on the current characteristics of a galaxy, but rather on its history. Nevertheless almost all

second derivatives were of the same order of magnitude. Figures 1–4 present the size of the second derivatives as a function of the size, mass, and type of the galaxy.

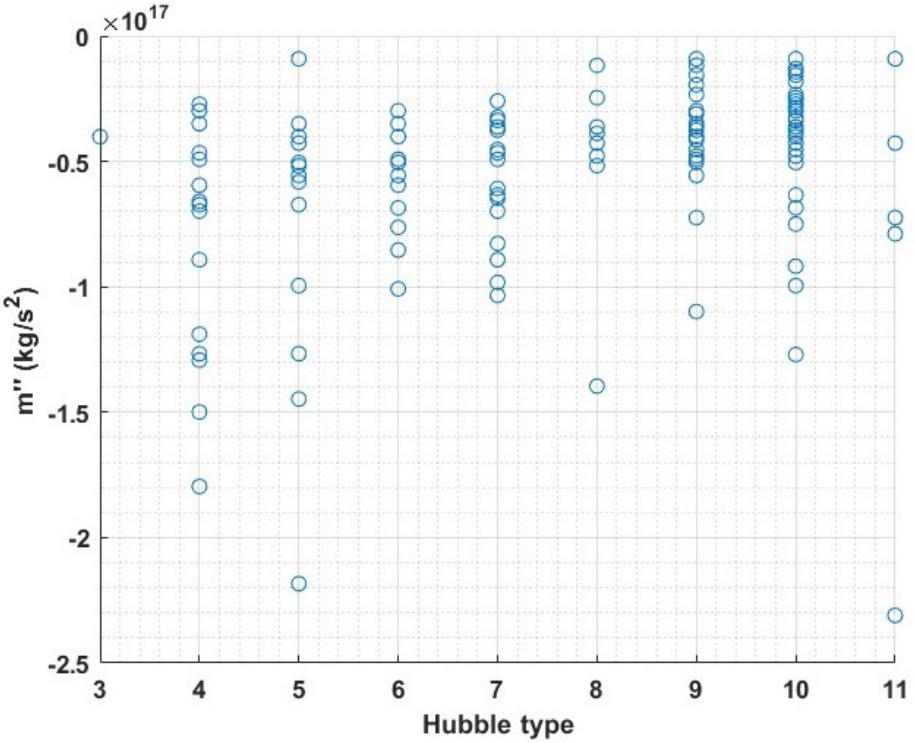

Figure 1. The size of the second derivative of the mass vs. Hubble type. 0—S0, 1—Sa, 2—Sab, 3—Sb, 4—Sbc, 5—Sc, 6—Scd, 7—Sd, 8—Sdm, 9—Sm, 10—Im and 11—BCD.

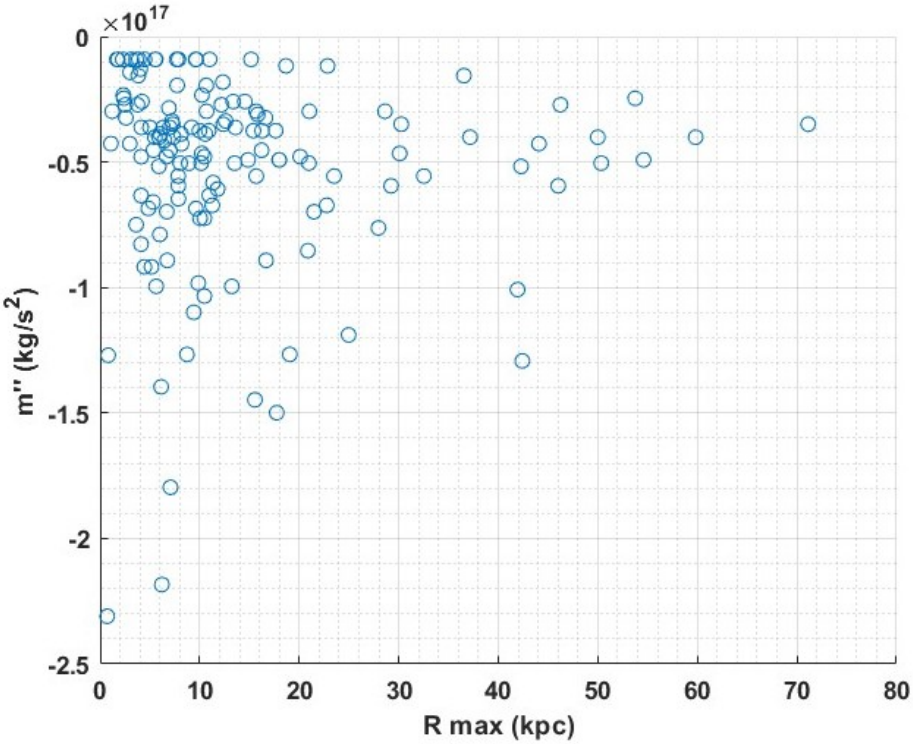

Figure 2. The size of the second derivative of the mass vs. the size of the galaxy.

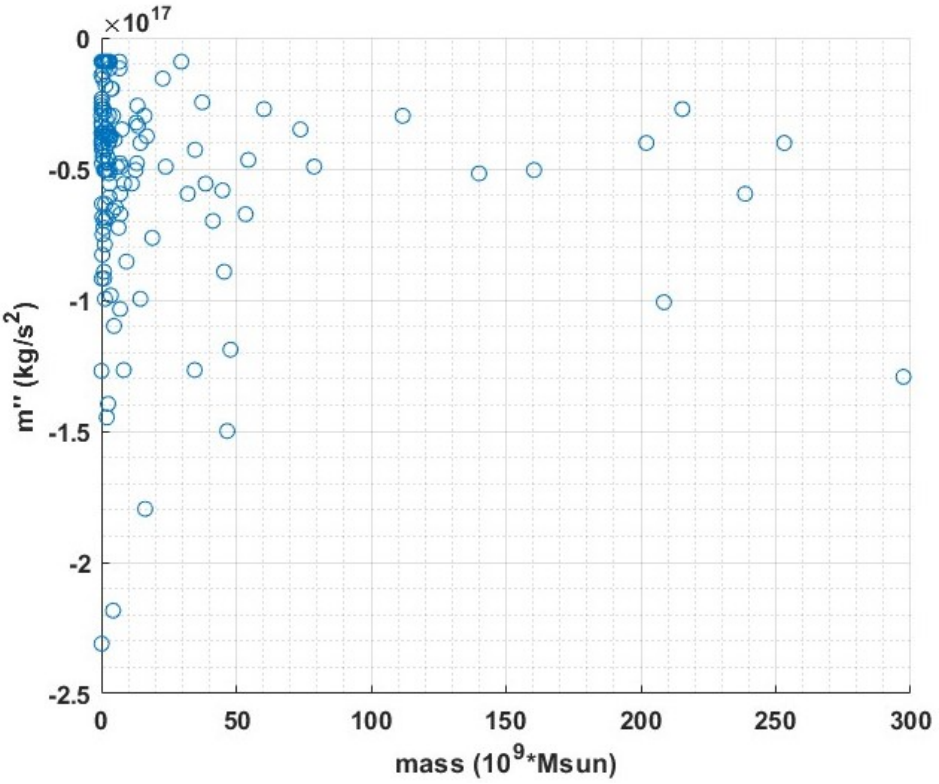

Figure 3. The size of the second derivative of the mass vs. galactic mass.

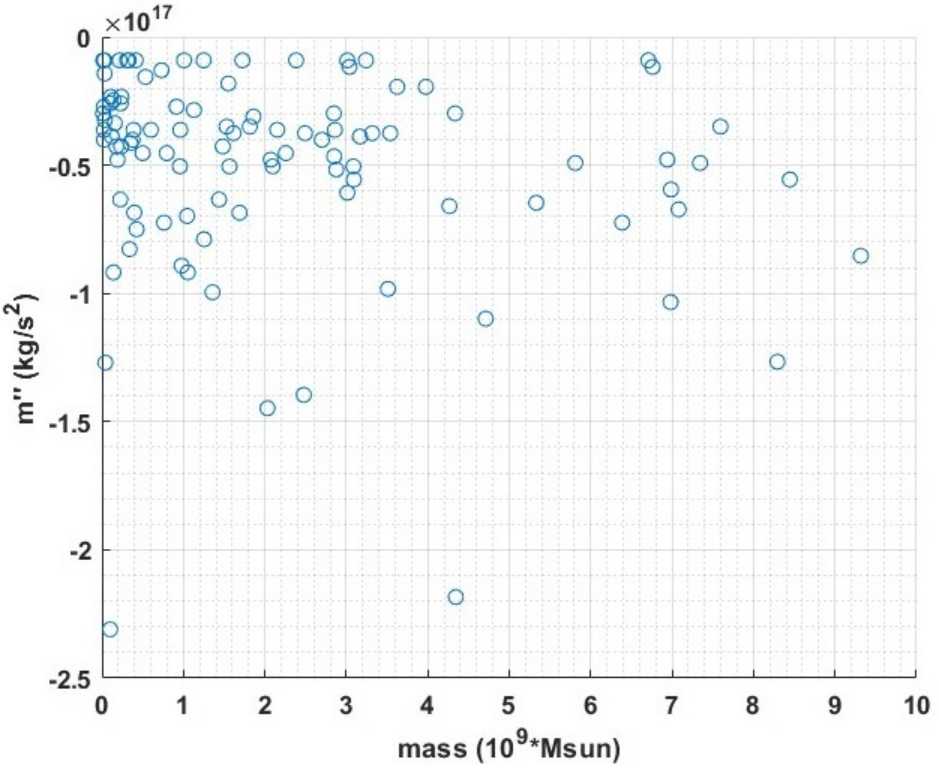

Figure 4. The size of the second derivative of the mass vs. galactic mass. Only galaxies with a mass smaller than $10^9 Msun$ are presented.

6. Conclusions

The Lorentz symmetry group excludes action at a distance potentials for the weak-field approximation; it follows that only retarded solutions are obtained. Retardation is

intuitively more significant when larger distances and larger second derivatives are present. We have demonstrated in [18] that the current approach does not require that the velocities in the system are high, as most galactic entities (stars, gas) are subluminal with $\frac{v}{c} \ll 1$. Typical velocities in galaxies are in the order of 100 km/s (see the figures above), which makes this ratio 0.001 or smaller. Notice, however, that every system has a retardation distance, beyond which retardation cannot be ignored. This follows from the fact that mass is exchanged between each natural system and its surroundings. For example, the solar wind in the solar system and on a much larger scale, galaxies that accrete intergalactic gas.

All gravitating systems must have a finite retardation distance. The question is, thus, quantitative. The change in mass of the Sun is minute, and thus, the retardation distance of the solar system is much larger than the size of the system, allowing us to neglect retardation effects. However, in galaxies the situation might be different. Since a the nature of the second derivative of the mass (i.e., the free parameter) is currently unknown, the possibility of having a relevant retardation distance cannot be ruled out. In [18], we demonstrated that the required values for the second derivative are consistent with current observational knowledge of galactic and extragalactic material content and dynamics. Of course, $|\ddot{M}|$ cannot be constant over the entire life time of the galaxy; for a simple model based on intergalactic mass depletion, see [18].

We emphasize that provided that the mass external to the galaxy is abundant (or totally depleted), $\ddot{M} \simeq 0$ and the retardation force is null. In this case, no "missing mass" phenomenon is expected. This was found in [42] for NGC1052-DF2 and for a few more ultra-diffuse galaxies.

Moreover, a recent paper [43] (see also [44–46]) states that "Recent measurements of gas velocity in the outer parts of high redshift galaxies suggest that steeply falling rotation curves may be common, or even universal, in these galaxies, in contrast to the near universal flat, non-declining rotation curves in nearby galaxies". This is in line with the claim of [18], which suggested that gas depletion is the source of the large $\ddot{M}$, and thus, an older galaxy should not have a significantly smaller $\ddot{M}$, which means steep rotation curves instead of flat rotation curves. Moreover, the paper states the following: "As soon as a smooth stellar disc is formed in the baryonic matter, with properties similar to the observed high redshift galaxies, the computed rotation curves are, without exception, relatively flat to large radius in the gas disc. Only a simulation without a dark matter halo is able to reproduce the observed rotation curves". This is in line with our theory, which questions the existence of dark matter. Furthermore, the paper states that "It would also imply that for these galaxies the flat rotation curves at low redshift must be due to dark matter which has subsequently fallen into the galactic potential well, or there must be some other explanation for their contemporary flat rotation curves, other than dark matter". Indeed, there is another explanation having to do with retardation.

According to an excellent paper by Kamada et al. [47], the velocity curves of spiral galaxies demonstrate a diversity that has been difficult to comprehend in the cold dark matter (CDM) approach. It was shown that in order to describe the data properly, one needs to introduce self-interacting dark matter (SIDM), which fits the velocity curves of galaxies with asymptotic velocities in the range of 25–300 km/s, which is the full interval of velocity diversity. The authors assumed a halo concentration–mass relation derived from the CDM model and a given self-interaction cross-section. For dark-matter-dominated galaxies, thermal equilibrium is reached due to self-interactions, which also creates significant cores and reduces DM densities. In the opposite case, thermalization leads to denser and smaller cores in more massive galaxies, and thus, explains the flatness of the velocity curves of highly luminous galaxies at small radii. This shows that the impact of the baryons on the SIDM halo profile and the scatter from the history of halos, as revealed in the concentration–mass relation, can corroborate the rotation curve diversity of galaxies. In our approach, no dark matter was needed. The central part of the galactic rotation curve was determined by baryons alone through Newtonian gravity and not through their impact on the SIDM halo profile. This satisfies Occam's razor: a direct reason is preferable over a complex

reason involving additional elements. The external part of the rotation curve (anomalous rotation) depended on the point at which retardation forces became the same order as the Newtonian forces; this is connected to both the size of the Newtonian force (size and distribution of the mass density) and retardation force size dependent on $\ddot{M}$. Thus, diversity was connected to both elements (determining, for example, whether the rotation curve will reach an asymptote or continue to rise and where the turning point exactly is in the rotation curve), as we have shown for 143 galaxies. The internal slope can be explained based on Newtonian physics and the baryon distribution alone.

We note that (the recently discovered) gravitational radiation is also connected to the peculiar galactic rotation curves. The second-order expansion in Equation (4) is only valid for limited durations and limited radii (near field):

$$t < T_{max} \qquad R < c\, T_{max} \equiv R_{max} \tag{14}$$

This is reasonable since the rotation curve in galaxies is the same order of magnitude as the size of the galaxy itself. A different case in which the size of the object is much smaller than the distance to the observer will result in a different approximation, leading to the famous quadruple equation of gravitational radiation predicted by Einstein [2] and corroborated in 1993 by Russell A. Hulse and Joseph H. Taylor, Jr., for which they received the Nobel Prize. The Hulse–Taylor binary pulsar gave indirect evidence of gravitational waves. Later, on 11 February 2016, the LIGO and Virgo scientific collaboration declared direct observation of gravitational waves. The observation was made five months earlier, on 14 September 2015, using the Advanced LIGO detectors. These were caused by the merging of a binary black hole configuration [38]. Thus, we consider near-field gravitational radiation, while previous art considered the far field.

We notice that the retarded gravity effect, which is of the order $\frac{R^2}{(ct)^2}$, has to be larger than other post-Newtonian contributions, that is $\frac{R^2}{(ct)^2} > \frac{v^2}{c^2}$. Taking the typical velocities in galaxies to be $O(10^2)$ km/s and the typical distance to be $R = O(1)$ kpc, one obtains the constraint $t < 3 \times 10^{14}$ s $= 9 \times 10^6$ years. Indeed, Equation (14) states the existence of R_{max} and T_{max} for the maximal distances and durations for the current approximation to be valid. However, there are additional limitations that come from the neglect of post-Newtonian contributions (that may come from the geodesic equations). It thus follows that $T_{max} < 9 \times 10^6$ years in order to justify the neglect of other post-Newtonian terms. Fortunately, we only need to calculate the retarded potential for durations up to 2×10^5 years (or distances up to 2×10^5 light years), and thus, the approximation is still valid for our current needs. That is, R/c is tens of thousands of years but may be short with respect to the duration in which the galactic density considerably changes or the neglect of other post-Newtonian terms becomes unjustified.

To conclude, we would like to consider conformal gravity by Mannheim [28,29]. The approach practiced in this study leads to a Newtonian potential with an additional linear potential. Such potentials can also be obtained from different considerations in conformal gravity. The fits looked reasonable when treating the coefficient of the linear potential as a variable that changes from galaxy to galaxy; this element is not in line with conformal gravity, in which the coefficient of the linear potential is a new universal constant of nature. This can be easily explained with retardation theory, in which $\ddot{M}$ changes depending on specific conditions of various galaxies and the history of their creation.

Retardation theory's approach satisfies Occam's razor rule and does not affect observations that are beyond the near-field regime [20], and therefore, does not clash with GR theory and its observations. Most of the 143 galaxies that were modeled in this work fit quite well with only a simple approximation to retarded gravity; others may benefit from a more detailed modeling, as was done in [18]. Of course, in some cases, the cylindrical symmetry approximation that we assumed will not suffice.

Finally, this paper does not discuss dark matter in the cosmological context. This is left for future works. Retarded gravity suffices to describe dark matter phenomena in the

close universe (anomalous galactic rotation curves and the Tully–Fisher relations, as well as anomalous masses obtained from gravitational lensing observations and from virial theorem calculations). However, it is not suitable for implementation in cosmological scales without modifications since retarded gravity is only obtained in a weak-field approximation to general relativity, in which the background metric is Lorentzian. There was an initial attempt to study a perturbation correction to the Friedman–Robertson–Walker metric (see [48]) suitable for cosmological scales; this is a problem that is, of course, closely connected to the spatial spectrum of the cosmic microwave background (CMB); the baryonic acoustic oscillations (BAO); the formation of large-scale structure (LSS); and eventually, to the formation of galaxies. However, much work still needs to be done in order to develop this approach and compare it with relevant data. We notice that for cosmological problems, it does not suffice to include one component ("dark matter") but also a second component ("dark energy"), where both are needed for the ΛCDM cosmology to fit data. Hence, a "weak-field" correction to a cosmological metric must explain both components. Indeed, retardation effects can increase or decrease gravity depending on the accelerations and velocities of matter components in the inhomogeneities that are formed in the primordial uniform universe; nothing specific can be said before making detailed calculations, and thus, this is left as a task for the future.

Recently, it was suggested in two remarkable papers [49,50] that the velocity of light in a vacuum and the universal gravitational constant are in fact dependent on time, and thus, are not universal (in the sense that in every epoch, they take different values). The new model is described by a modified Friedman–Robertson–Walker metric and leads to new equations that allow for obtaining dark-energy-like effects but without postulating dark energy. In [49], it is shown that in such a model, the universe should be much older, explaining the distant galaxies that were recently discovered by the James Webb Space Telescope (JWST) and their mature state, which is not compatible with the present ΛCDM cosmological model. The model fits the supernovae type 1a Pantheon+ data well, as well as the ΛCDM model. There is hope that this model is also consistent with the CMB spectrum, big bang nucleosynthesis of hydrogen and hellium, and other observations. It is easy to see that this model does not contradict the retardation model, which explains "dark matter" effects at a non-cosmological scale. Thus, the two models complement each other by explaining "dark matter" phenomena at different scales (local and cosmological). Moreover, a perturbation approach around the CCC+TL cosmology [49,50] metric (and not around a Lorentz metric, which is the retarded gravity approach described in the current paper) may be helpful in obtaining the missing pieces of the puzzle, such as the CMB power spectrum.

Author Contributions: Conceptualization, A.Y.; methodology, A.Y. and T.Z.; software, Y.G. and T.Z.; formal analysis, A.Y.; investigation, Y.G. and T.Z.; writing—original draft preparation, Y.G. and T.Z.; writing—review and editing, A.Y. and T.Z.; visualization, Y.G. and T.Z.; supervision, A.Y.; project administration, A.Y. All authors have read and agreed to the published version of the manuscript.

Funding: This research received no external funding.

Data Availability Statement: The data underlying this article are available at http://astroweb.cwru.edu/SPARC/ (accessed on 12 March 2024). It includes extended 21-cm rotation curves as well as B-band photometry for the sample of galaxies analyzed in this work.

Conflicts of Interest: The authors declare no conflicts of interest.

Appendix A. Representative Galaxy Fits

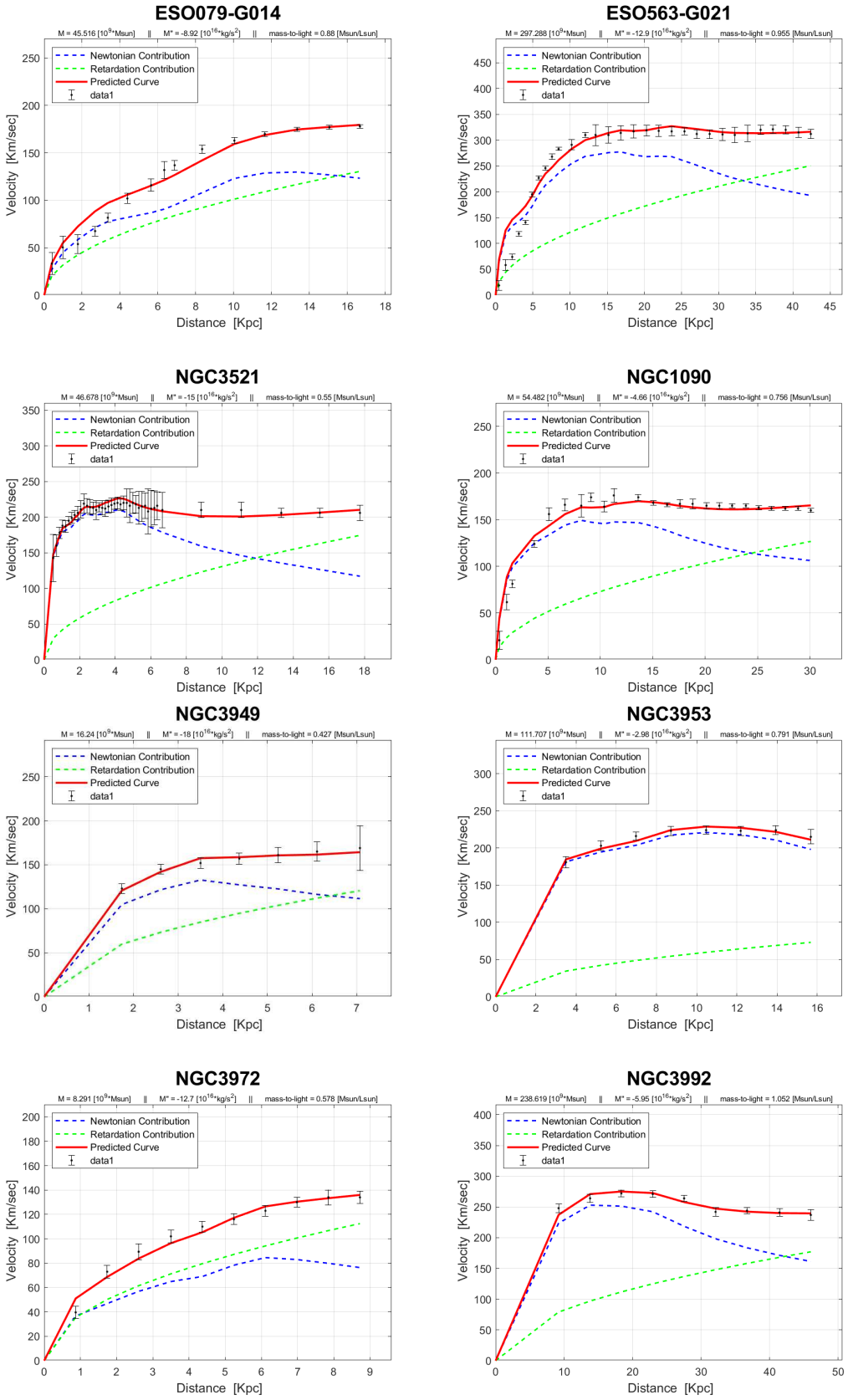

Figure A1. The rotation curves of "Sbc"-type galaxies.

Appendix B. Galaxy Data Tables

In the following, we use the following numbering scheme for the Hubble galaxy types: 0—S0, 1—Sa, 2—Sab, 3—Sb, 4—Sbc, 5—Sc, 6—Scd, 7—Sd, 8—Sdm, 9—Sm, 10—Im and 11—BCD.

Galaxy Name	HubbleType	Distance (Mpc)	Derror (Mpc)	Red Shift ($z=H_0 D/c$)	R_{max} (Kpc)	ddM (kg s^{-2})	Γ ($M_\odot/L_\odot$)	Total Luminosity ($10^9 L_\odot$)	Mass ($10^9 M_{sun}$)
'UGCA444'	10	0.98	0.05	0.000226602	2.59	-3.24E+16	3	0.012	0.036
'NGC3109'	9	1.33	0.07	0.000307531	6.45	-4.14E+16	1.8	0.194	0.3492
'NGC0300'	7	2.08	0.1	0.000480951	11.8	-6.0787E+16	1.030901288	2.922	3.012293562
'NGC0055'	9	2.11	0.11	0.000487888	13.5	-5.04536E+16	0.206866953	4.628	0.957380258
'UGC07577'	10	2.59	0.13	0.000598877	1.68	-9.12E+15	0.496	0.045	0.02232
'UGC07232'	10	2.83	0.17	0.000654371	0.81	-1.27E+17	0.369	0.113	0.041697
'NGC4214'	10	2.87	0.14	0.00066362	5.63	-9.95372E+16	1.188841202	1.141	1.356467811
'NGC2403'	6	3.16	0.16	0.000730676	20.87	-8.53288E+16	0.927896996	10.041	9.317013734
'NGC3741'	10	3.21	0.17	0.000742237	7	-3.62452E+16	0.879828326	0.028	0.024635193
'NGC2366'	10	3.27	0.16	0.000756111	6.03	-3.88E+16	0.5	0.236	0.118
'UGC04483'	10	3.34	0.31	0.000772297	1.21	-2.97868E+16	0.996566524	0.013	0.012955365
'CamB'	10	3.36	0.26	0.000776921	1.79	-9.12E+15	0.2	0.075	0.015
'UGC04305'	10	3.45	0.17	0.000797732	5.52	-9.12E+15	0.4472103	0.736	0.329146781
'NGC6789'	11	3.52	0.18	0.000813918	0.71	-2.31E+17	1	0.1	0.1
'NGC2976'	5	3.58	0.18	0.000827791	2.27	-9.12E+15	0.893562232	3.371	3.012198283
'NGC7793'	7	3.61	0.18	0.000834728	7.87	-6.4662E+16	0.756223176	7.05	5.331373391
'NGC0247'	7	3.7	0.19	0.000855539	14.54	-2.59118E+16	1.827467811	7.332	13.39899399
'IC2574'	9	3.91	0.2	0.000904096	10.23	-2.33284E+16	0.234334764	1.016	0.23808412
'DDO154'	10	4.04	0.2	0.000934156	5.92	-4.01202E+16	0.481545064	0.053	0.025521888
'NGC2915'	11	4.06	0.2	0.00093878	10.04	-7.2412E+16	1.188841202	0.641	0.76204721
'DDO168'	10	4.25	0.21	0.000982713	4.12	-4.79E+16	1	0.191	0.191
'UGCA442'	9	4.35	0.22	0.001005836	6.33	-3.62452E+16	2.768240343	0.14	0.387553648
'NGC4068'	10	4.37	0.22	0.00101046	2.37	-2.46E+16	0.6	0.236	0.1416
'UGC07866'	10	4.57	0.23	0.001056706	2.32	-2.33284E+16	0.872961373	0.124	0.10824721
'UGC08490'	9	4.65	0.53	0.001075204	10.15	-5.04536E+16	2.060944206	1.017	2.095980258
'UGC07603'	7	4.7	1.41	0.001086765	4.11	-8.27454E+16	0.900429185	0.376	0.338561373
'UGC07524'	9	4.74	0.24	0.001096014	10.69	-2.97868E+16	1.779399142	2.436	4.334616309
'ESO444-G084'	10	4.83	0.48	0.001116825	4.44	-9.17871E+16	1.985407725	0.071	0.140963948
'UGC07559'	10	4.97	0.25	0.001149196	2.53	-2.72034E+16	0.206866953	0.109	0.022548498
'UGC01281'	8	5.27	0.24	0.001218564	5	-3.62452E+16	1.7	0.353	0.6001
'UGCA281'	11	5.68	0.28	0.001313367	1.08	-4.27035E+16	0.91416309	0.194	0.177347639
'NGC1705'	11	5.73	0.29	0.001324929	6	-7.88704E+16	2.349356223	0.533	1.252206867
'UGC05721'	7	6.18	1.85	0.001428981	6.74	-8.92038E+16	1.841201717	0.531	0.977678112
'NGC6503'	6	6.26	0.31	0.001447479	23.5	-5.56203E+16	0.879828326	12.845	11.30139485
'UGC08286'	6	6.5	0.21	0.001502973	8.04	-5.04536E+16	2.459227468	1.255	3.086330472
'NGC2903'	4	6.6	1.98	0.001526096	24.96	-1.18912E+17	0.584549356	81.863	47.85296395
'UGC08550'	7	6.7	2	0.001549218	5.36	-4.52869E+16	1.724463519	0.289	0.498369957
'DDO064'	10	6.8	2.04	0.001572341	2.98	-4.27E+16	1.5	0.157	0.2355
'KK98-251'	10	6.8	2.04	0.001572341	3.13	-9.12E+15	2.541630901	0.085	0.216038627
'UGC07151'	6	6.87	0.34	0.001588527	5.5	-4.01202E+16	1.181974249	2.284	2.699629185
'UGC02455'	10	6.92	2.08	0.001600088	4.03	-1.2995E+16	0.2	3.649	0.7298
'NGC5585'	7	7.06	2.12	0.00163246	10.96	-6.33703E+16	0.488412017	2.943	1.437396567
'UGC08837'	10	7.21	0.36	0.001667144	4.2	-2.59118E+16	0.2	0.501	0.1002
'NGC0024'	5	7.3	0.36	0.001687954	11.27	-6.72453E+16	1.820600858	3.889	7.080316738
'UGC05764'	10	7.47	2.24	0.001727263	3.62	-7.49954E+16	5	0.085	0.425
'DDO161'	10	7.5	2.25	0.0017342	13.37	-2.59118E+16	0.419742489	0.548	0.230018884
'UGC05918'	10	7.66	2.3	0.001771196	4.46	-9.12E+15	4.327038627	0.233	1.0082
'NGC3521'	4	7.7	2.3	0.001780445	17.74	-1.49912E+17	0.550214592	84.836	46.67800515
'D631-7'	10	7.72	0.18	0.00178507	7.23	-3.36618E+16	0.8	0.196	0.1568

Figure A2. Table of galaxies and their properties that were modeled in this work—part 1.

Galaxy Name	HubbleType	Distance (Mpc)	Derror (Mpc)	Red Shift ($z=H_0 D/c$)	R_{max} (Kpc)	ddM (kg s^{-2})	Γ ($M_\odot/L_\odot$)	Total Luminosity ($10^9 L_\odot$)	Mass ($10^9 M_{sun}$)
'UGC07323'	8	8	2.4	0.001849813	5.9	-5.17E+16	0.7	4.109	2.8763
'UGC07690'	10	8.11	2.43	0.001875248	4.13	-3.62452E+16	1.120171674	0.858	0.961107296
'UGC07608'	10	8.21	2.46	0.001898371	4.85	-6.85E+16	1.5	0.264	0.396
'UGC07399'	8	8.43	2.53	0.00194924	6.13	-1.39579E+17	2.143347639	1.156	2.477709871
'UGC05986'	9	8.63	2.59	0.001995486	9.41	-1.09871E+17	1.003433476	4.695	4.711120172
'UGC05829'	10	8.64	2.59	0.001997798	6.91	-2.85E+16	2	0.564	1.128
'D564-8'	10	8.79	0.28	0.002032482	3	-1.42867E+16	1	0.033	0.033
'NGC4559'	6	9	2.7	0.00208104	20.97	-5.04536E+16	0.653218884	19.377	12.65742232
'UGC05414'	10	9.4	2.82	0.00217353	4.11	-6.33703E+16	0.2	1.123	0.2246
'UGC04278'	7	9.51	2.85	0.002198965	6.7	-6.98E+16	0.8	1.307	1.0456
'UGC04325'	9	9.6	2.88	0.002219776	5.59	-9.12E+15	3.310729614	2.026	6.707538197
'UGC12632'	9	9.77	2.93	0.002259084	10.66	-1.94534E+16	3.056652361	1.301	3.976704721
'NGC5055'	4	9.9	0.3	0.002289144	54.59	-4.91619E+16	0.515879828	152.922	78.88937511
'UGC00891'	9	10.2	3.1	0.002358512	7.39	-4.01E+16	1	0.374	0.374
'UGC02023'	10	10.4	3.1	0.002404757	3.76	-2.72E+16	0.7	1.308	0.9156
'UGC02259'	8	10.5	3.1	0.00242788	8.14	-3.88285E+16	2.878111588	1.725	4.964742489
'UGC09992'	10	10.7	3.21	0.002474125	3.89	-9.12E+15	1.230042918	0.336	0.413294421
'NGC1003'	6	11.4	3.42	0.002635984	30.24	-3.49535E+16	1.113304721	6.82	7.592738197
'UGC06446'	7	12	3.6	0.00277472	10.22	-4.65785E+16	2.884978541	0.988	2.850358798
'UGC00731'	10	12.5	3.75	0.002890333	10.91	-3.75368E+16	5	0.323	1.615
'UGC04499'	8	12.5	3.75	0.002890333	8.18	-4.27035E+16	0.955364807	1.552	1.48272618
'ESO116-G012'	7	13	3.9	0.003005946	9.86	-9.82455E+16	0.818025751	4.292	3.510966524
'UGC07261'	8	13.1	3.93	0.003029069	6.67	-4.78702E+16	1.181974249	1.753	2.072000858
'UGC12732'	9	13.2	4	0.003052192	15.4	-3.75368E+16	2.122746781	1.667	3.538618884
'NGC0100'	6	13.5	4.05	0.00312156	9.62	-6.8537E+16	0.522746781	3.232	1.689517597
'PGC51017'	11	13.6	1.4	0.003144682	3.63	-9.12E+15	0.2	0.155	0.031
'NGC3198'	5	13.8	1.4	0.003190928	44.08	-4.27035E+16	0.907296137	38.279	34.73038884
'UGC06628'	9	15.1	4.53	0.003491522	7.69	-9.12E+15	0.460944206	3.739	1.723470386
'D512-2'	10	15.2	4.56	0.003514645	3.83	-1.55784E+16	1.642060086	0.325	0.533669528
'UGC10310'	9	15.2	4.6	0.003514645	7.74	-1.94534E+16	2.081545064	1.741	3.623969957
'DDO170'	10	15.4	4.62	0.00356089	12.33	-1.81617E+16	2.85751073	0.543	1.551628326
'NGC6015'	6	17	5.1	0.003930853	29.23	-5.94953E+16	0.996566524	32.129	32.01868584
'UGC00191'	9	17.1	5.1	0.003953975	9.98	-3.75368E+16	1.655793991	2.004	3.318211159
'NGC5907'	5	17.3	0.9	0.004000221	50.33	-5.04536E+16	0.91416309	175.425	160.3670601
'NGC3726'	5	18	2.5	0.004162079	32.52	-5.56203E+16	0.550214592	70.234	38.64377167
'NGC3769'	3	18	2.5	0.004162079	37.16	-4.01202E+16	0.776824034	18.679	14.51029614
'NGC3877'	5	18	2.5	0.004162079	11.35	-5.82036E+16	0.61888412	72.535	44.89075966
'NGC3893'	5	18	2.5	0.004162079	19.05	-1.26662E+17	0.591416309	58.525	34.61263948
'NGC3917'	6	18	2.5	0.004162079	14.86	-4.91619E+16	1.08583691	21.966	23.85149356
'NGC3949'	4	18	2.5	0.004162079	7.07	-1.79621E+17	0.426609442	38.067	16.23974163
'NGC3953'	4	18	2.5	0.004162079	15.68	-2.97868E+16	0.79055794	141.301	111.7066275
'NGC3972'	4	18	2.5	0.004162079	8.72	-1.26662E+17	0.577682403	14.353	8.291475536
'NGC4010'	7	18	2.5	0.004162079	10.47	-1.03412E+17	0.406008584	17.193	6.980505579
'NGC4051'	4	18	2.5	0.004162079	12.19	-2.72034E+16	0.632618026	95.268	60.26825408
'NGC4085'	5	18	2.5	0.004162079	6.2	-2.18371E+17	0.2	21.724	4.3448
'NGC4088'	4	18	2.5	0.004162079	21.48	-6.98287E+16	0.385407725	107.286	41.34885322
'NGC4100'	4	18	2.5	0.004162079	22.76	-6.72453E+16	0.900429185	59.394	53.48009099
'NGC4183'	6	18	2.5	0.004162079	21.02	-2.97868E+16	1.477253219	10.838	16.01047039
'NGC4389'	4	18	2.5	0.004162079	5.32	-6.59536E+16	0.2	21.328	4.2656

Figure A3. Table of galaxies and their properties that were modeled in this work—part 2.

Galaxy Name	HubbleType	Distance (Mpc)	Derror (Mpc)	Red Shift ($z=H_0 D/c$)	R_{max} (Kpc)	ddM (kg s^{-2})	Γ ($M_\odot/L_\odot$)	Total Luminosity ($10^9 L_\odot$)	Mass ($10^9 M_{sun}$)
'UGC06399'	9	18	2.5	0.004162079	7.85	-5.56203E+16	1.346781116	2.296	3.092209442
'UGC06667'	6	18	2.5	0.004162079	7.85	-5.94953E+16	5	1.397	6.985
'UGC06818'	9	18	2.5	0.004162079	7.01	-4.53E+16	0.5	1.588	0.794
'UGC06917'	9	18	2.5	0.004162079	10.47	-7.2412E+16	0.934763948	6.832	6.386307296
'UGC06923'	10	18	2.5	0.004162079	5.16	-9.17871E+16	0.364806867	2.89	1.054291845
'UGC06930'	7	18	2.5	0.004162079	16.61	-3.23701E+16	1.449785408	8.932	12.94948326
'UGC06983'	6	18	2.5	0.004162079	15.68	-5.56203E+16	1.593991416	5.298	8.444966524
'UGC07089'	8	18	2.5	0.004162079	9.18	-3.62E+16	0.6	3.585	2.151
'UGC11820'	9	18.1	5.43	0.004185202	15.82	-3.10785E+16	1.916738197	0.97	1.859236052
'UGC07125'	9	19.8	5.9	0.004578287	18.68	-1.17033E+16	1.120171674	2.712	3.037905579
'NGC0289'	4	20.8	5.2	0.004809514	71.12	-3.49535E+16	1.024034335	72.065	73.79703433
'UGC05716'	9	21.3	5.3	0.004925127	12.37	-3.49535E+16	2.603433476	0.588	1.530818884
'NGC3992'	4	23.7	2.3	0.005480071	46.02	-5.94953E+16	1.051502146	226.932	238.619485
'UGC11557'	8	24.2	6.05	0.005595684	10.56	-3.88285E+16	0.261802575	12.101	3.168072961
'ESO079-G014'	4	28.7	7.17	0.006636204	16.67	-8.92038E+16	0.879828326	51.733	45.5161588
'UGC00634'	9	30.9	7.7	0.007144903	18.01	-4.91619E+16	1.944206009	2.989	5.81123176
'F583-1'	9	35.4	8.85	0.008185423	16.26	-3.75368E+16	2.527896996	0.986	2.492506438
'NGC1090'	4	37	9.25	0.008555385	30.09	-4.65785E+16	0.756223176	72.045	54.48209871
'NGC5371'	4	39.7	9.92	0.009179697	46.24	-2.72034E+16	0.632618026	340.393	215.3387476
'UGC05999'	10	47.7	9.5	0.01102951	16.22	-4.52869E+16	0.66695279	3.384	2.25696824
'F563-1'	9	48.9	9.8	0.011306982	20.1	-4.78702E+16	3.6472103	1.903	6.940641202
'F565-V2'	10	51.8	10.4	0.011977539	8.91	-5.05E+16	2.8	0.559	1.5652
'F571-8'	5	53.3	10.7	0.012324379	15.55	-1.44746E+17	0.2	10.164	2.0328
'F583-4'	5	53.3	10.7	0.012324379	7.29	-3.49535E+16	1.058369099	1.715	1.815103004
'UGC01230'	9	53.7	10.7	0.01241687	36.54	-1.55784E+16	2.987982833	7.62	22.76842918
'UGC05005'	10	53.7	10.7	0.01241687	28.61	-2.97868E+16	0.694420601	4.1	2.847124464
'F563-V1'	10	54	10.8	0.012486238	7.87	-9.12E+15	0.2	1.54	0.308
'UGC05750'	8	58.7	11.7	0.013573003	22.85	-1.17033E+16	2.026609442	3.336	6.760769099
'F563-V2'	10	59.7	11.9	0.01380423	10.47	-4.78702E+16	4.40944206	2.986	13.16659399
'ESO563-G021'	4	60.8	9.1	0.014058579	42.41	-1.29246E+17	0.955364807	311.177	297.2875545
'UGC00128'	8	64.5	9.7	0.014914118	53.75	-2.46201E+16	3.111587983	12.02	37.40128755
'F561-1'	9	66.4	10	0.015353448	9.66	-9.12E+15	0.584549356	4.077	2.383207725
'NGC2998'	5	68.1	10.2	0.015746534	42.28	-5.17452E+16	0.927896996	150.902	140.0215124
'UGC11455'	6	78.6	11.8	0.018174413	41.93	-1.00829E+17	0.557081545	374.322	208.5278781
'F567-2'	9	79	11.8	0.018266904	9.59	-9.12E+15	1.518454936	2.134	3.240382833
'F571-V1'	7	80.1	8	0.018521253	13.59	-3.62452E+16	1.545922747	1.849	2.858411159
'F568-V1'	7	80.6	8.06	0.018636866	17.63	-3.75368E+16	4.402575107	3.825	16.83984979
'NGC0801'	5	80.7	8.07	0.018659989	59.82	-4.01202E+16	0.646351931	312.57	202.0302232
'F568-3'	7	82.4	8.24	0.019053074	17.98	-4.91619E+16	0.879828326	8.346	7.34304721
'UGC09037'	6	83.6	8.4	0.019330546	27.96	-7.6287E+16	0.275536481	68.614	18.90566009
'F574-2'	9	89.1	8.91	0.020602293	11	-9.12E+15	0.434	2.877	1.248618
'F579-V1'	5	89.5	8.95	0.020694783	15.16	-9.12E+15	2.500429185	11.848	29.62508498
'F568-1'	5	90.7	9.7	0.020972255	13.23	-9.95372E+16	2.315021459	6.252	14.47351416
'F574-1'	7	96.8	9.68	0.022382738	12.6	-3.36618E+16	2.074678112	6.537	13.56217082
'UGC12506'	6	100.6	10.1	0.023261399	49.99	-4.01202E+16	1.813733906	139.571	253.1446549

Figure A4. Table of galaxies and their properties that were modeled in this work—part 3.

References

1. Eddington, A.S. *The Mathematical Theory of Relativity*; Cambridge University Press: Cambridge, UK, 1923.
2. Einstein, A. *Sitzungsberichte der Königlich Preussischen Akademie der Wissenschaften Berlin*; Part 1; The Prusssian Academy of Sciences: Berlin, Germany, 1916; pp. 688–696.
3. Misner, C.W.; Thorne, K.S.; Wheeler, J.A. *Gravitation*; W.H. Freeman & Company: New York, NY, USA, 1973.
4. Narlikar, J.V. *Introduction to Cosmology*, 2nd ed.; Cambridge University Press: Cambridge, UK, 1993.
5. Weinberg, S. *Gravitation and Cosmology: Principles and Applications of the General Theory of Relativity*; John Wiley & Sons, Inc.: Hoboken, NJ, USA, 1972.
6. de Swart, J.G.; Bertone, G.; van Dongen, J. How dark matter came to matter. *Nat. Astron.* **2017**, *1*, 0059. [CrossRef]
7. Zwicky, F. On a new cluster of nebulae in Pisces. *Proc. Natl. Acad. Sci. USA* **1937**, *23*, 251–256. [CrossRef] [PubMed]
8. Yahalom, A. The virial theorem for retarded gravity. *Int. J. Mod. Phys. D* **2023**, *32*, 2342013. [CrossRef]
9. Volders L.M.J.S. Neutral hydrogen in M 33 and M 101. *Bull. Astr. Inst. Netherl.* **1959**, *14*, 323.
10. Rubin, V.C.; Ford, W.K., Jr. Rotation of the Andromeda nebula from a spectroscopic survey of emission regions. *Astrophys. J.* **1970**, *159*, 379. [CrossRef]
11. Rubin, V.C.; Ford, W.K., Jr.; Thonnard, N. Extended rotation curves of high-luminosity spiral galaxies. IV-Systematic dynamical properties, SA through SC. *Astrophys. J.* **1978**, *225*, L107–L111. [CrossRef]
12. Rubin, V.C.; Ford, W.K., Jr.; Thonnard, N. Rotational properties of 21 SC galaxies with a large range of luminosities and radii, from NGC 4605/R = 4 kpc/to UGC 2885/R = 122 kpc. *Astrophys. J.* **1980**, *238*, 471–487. [CrossRef]
13. Bosma, A. 21-cm line studies of spiral galaxies. II. The distribution and kinematics of neutral hydrogen in spiral galaxies of various morphological types. *Astrophys. J.* **1981**, *86*, 1825–1846. [CrossRef]
14. Sofue, Y.; Rubin, V.C. Rotation curves of spiral galaxies. *Ann. Rev. Astron. Astrophys.* **2001**, *39*, 137–174. [CrossRef]
15. de Bloc, W.J.G.; Walter, F.; Brinks, E.; Trachternach, C.; Oh, S.H.; Kennicutt, R.C. High-resolution rotation curves and galaxy mass models from THINGS. *Astrophys. J.* **2008**, *136*, 2648. [CrossRef]
16. Wagman, M. Retardation Theory in Galaxies. Ph.D. Thesis, Senate of Ariel University, Samria, Israel, 23 September 2019.
17. Wagman, M.; Horwitz, L.P.; Yahalom, A. Applying Retardation Theory to Galaxies. *J. Phys. Conf. Ser.* **2023**, *2482*, 012005. [CrossRef]
18. Yahalom, A. Lorentz Symmetry Group, Retardation, Intergalactic Mass Depletion and Mechanisms Leading to Galactic Rotation Curves. *Symmetry* **2020**, *12*, 1693. [CrossRef]
19. Yahalom, A. The Cosmological Decrease of Galactic Density and the Induced Retarded Gravity Effect on Rotation Curves. *J. Phys. Conf. Ser.* **2021**, *1956*, 012002. [CrossRef]
20. Yahalom, A. Effects of Higher Order Retarded Gravity. *Universe* **2021**, *7*, 207. [CrossRef]
21. Yahalom, A. Lensing Effects in Retarded Gravity. *Symmetry* **2021**, *13*, 1062. [CrossRef]
22. Tully, R.B.; Fisher, J.R. A new method of determining distances to galaxies. *Astron. Astrophys.* **1977**, *54*, 661–673.
23. Yahalom, A. Tully–Fisher relations and retardation theory for galaxies. *Int. J. Mod. Phys. D* **2021**, *30*, 2142008. [CrossRef]

24. Yahalom, A. Lensing effects in galactic retarded gravity: Why "Dark Matter" is the same for both gravitational lensing and rotation curves. *Int. J. Mod. Phys. D* **2022**, *31*, 2242018. [CrossRef]
25. Navarro, J.F.; Frenk, C.S.; White, S.D.M. The Structure of Cold Dark Matter Halos. *Astrophys. J.* **1996**, *462*, 563–575. [CrossRef]
26. Sancisi, R. The visible matter—Dark matter coupling. In Proceedings of the IAU Symposium 220, "Dark Matter in Galaxies", Sydney, Australia, 21–25 July 2003.
27. Milgrom, M. A modification of the Newtonian dynamics as a possible alternative to the hidden mass hypothesis. *Astrophys. J.* **1983**, *270*, 365–370. [CrossRef]
28. Mannheim, P.D. Linear potentials and galactic rotation curves. *Astrophys. J.* **1993**, *419*, 150. [CrossRef]
29. Mannheim, P.D. Local and global gravity. *Found. Phys.* **1996**, *26*, 1683–1709. [CrossRef]
30. Moffat, J.W. Scalar–tensor–vector gravity theory. *J. Cosmol. Astropart. Phys.* **2006**, *3*, 4. [CrossRef]
31. Yahalom, A. MOND & Retarded Gravity. *Bulg. J. Phys.* **2023**, *50*, 1–16.
32. Landau, L.D. *The Classical Theory of Fields*, 4th ed.; Pergamon: Oxford, UK, 1975.
33. Jackson, J.D. *Classical Electrodynamics*, 3rd ed.; Wiley: New York, NY, USA, 1999.
34. Schwinger, J.; Lester, L.; DeRaad, K.W., Jr. *Classical Electrodynamics, Advanced Book Program*; Perseus Books: Reading, MA, USA, 1998.
35. Yahalom, A. The geometrical meaning of time. *Found. Phys.* **2008**, *38*, 489–497. [CrossRef]
36. Yahalom, A. The Gravitational Origin of the Distinction between Space and Time. *Int. J. Mod. Phys. D* **2009**, *18*, 2155–2158. [CrossRef]
37. Abbott, B.P.; Abbott, R.; Abbott, T.D.; Abernathy, M.R.; Acernese, F.; Ackley, K.; Adams, C.; Adams, T.; Addesso, P.; Adhikari, R.X.; et al. Directly comparing GW150914 with numerical solutions of Einstein's equations for binary black hole coalescence. *Phys. Rev. D* **2016**, *94*, 064035. [CrossRef]
38. Castelvecchi, D.; Witze, W. Einstein's gravitational waves found at last. *Nat. News* **2016**. [CrossRef]
39. Feynman, R.P.; Leighton, R.B.; Sands, M.L. *Feynman Lectures on Physics*, revised 50th anniversary ed.; Basic Books: New York, NY, USA, 2011.
40. McGaugh, S. McGaugh's Data Pages. N.p., n.d. 2017. Available online: http://astroweb.case.edu/ssm/data/ (accessed on 22 January 2017).
41. Sanders, R.; McGaugh, S. Modified Newtonian dynamics as an alternative to dark matter. *Annu. Rev. Astron. Astrophys.* **2002**, *40*, 263–317. [CrossRef]
42. van Dokkum, P.; Danieli, S.; Cohen, Y.; Merritt, A.; Romanowsky, A.J.; Abraham, R.; Brodie, J.; Conroy, C.; Lokhorst, D.; Mowla, L.; et al. A galaxy lacking dark matter. *Nature* **2018**, *555*, 629–632. [CrossRef] [PubMed]
43. Nelson, A.H.; Williams, P.R. Recent Observations of the Rotation of Distant Galaxies and the Implication for Dark Matter. *arXiv* **2024**, arXiv:2401.13783.
44. Genzel, R.; Schreiber, N.F.; Übler, H.; Lang, P.; Naab, T.; Bender, R.; Tacconi, L.J.; Wisnioski, E.; Wuyts, S.; Alexander, T.; et al. Strongly baryon-dominated disk galaxies at the peak of galaxy formation ten billion years ago. *Nature* **2017**, *543*, 397–401. [CrossRef] [PubMed]
45. Lang, P.; Schreiber, N.M.; Genzel, R.; Wuyts, S.; Wisnioski, E.; Beifiori, A.; Belli, S.; Bender, R.; Brammer, G.; Burkert, A.; et al. Falling outer rotation curves of star-forming galaxies at $0.6 \lesssim Z \lesssim 2.6$ probed with KMOS3D and SINS/ZC-SINF. *Astrophys. J.* **2017**, *840*, 92. [CrossRef]
46. Lang, P. Falling rotation curves of star-forming galaxies at z = 0.7–2.6 probed with KMOS-3D and SINS/zC-SINF. In Proceedings of the KMOS@5 Workshop, ESO Garching, Garching bei München, Germany, 3–6 December 2018. [CrossRef]
47. Kamada, A.; Kaplinghat, M.; Pace, A.B.; Yu, H.B. Self-Interacting Dark Matter Can Explain Diverse Galactic Rotation Curves. *Phys. Rev. Lett.* **2017**, *119*, 111102. [CrossRef] [PubMed]
48. Yahalom, A. Gravity, stability and cosmological models. *Int. J. Mod. Phys. D* **2017**, *26*, 1743026. [CrossRef]
49. Gupta, R.P. *JWST* early Universe observations and ΛCDM cosmology *Mon. Not. R. Astron. Soc.* **2023**, *524*, 3385–3395. [CrossRef]
50. Gupta, R.P. Testing CCC+ TL Cosmology with Observed BAO Features. *arXiv* **2024**, arXiv:2401.09483.